

Dense open-set recognition based on training with noisy negative images

Petra Bevandić, Ivan Krešo, Marin Oršić, and Siniša Šegvić

Faculty of Electrical Engineering and Computing, University of Zagreb, Croatia

Abstract

Deep convolutional models often produce inadequate predictions for inputs which are foreign to the training distribution. Consequently, the problem of detecting outlier images has recently been receiving a lot of attention. Unlike most previous work, we address this problem in the dense prediction context. Our approach is based on two reasonable assumptions. First, we assume that the inlier dataset is related to some narrow application field (e.g. road driving). Second, we assume that there exists a general-purpose dataset which is much more diverse than the inlier dataset (e.g. ImageNet-1k). We consider pixels from the general-purpose dataset as noisy negative samples since most (but not all) of them are outliers. We encourage the model to recognize borders between the known and the unknown by pasting jittered negative patches over inlier training images. Our experiments target two dense open-set recognition benchmarks (WildDash 1 and Fishyscapes) and one dense open-set recognition dataset (StreetHazard). Extensive performance evaluation indicates competitive potential of the proposed approach.

Keywords: dense prediction, semantic segmentation, dense open-set recognition, outlier detection

1. Introduction

Deep convolutional approaches have recently achieved proficiency on realistic semantic segmentation datasets such as Vistas [1] or Ade20k [2]. This success has increased interest in exciting real-world applications such as autonomous driving [3] or medical diagnostics [4]. However, visual proficiency of the current state-of-the-art models is still insufficient to accommodate the demanding requirements of these applications [5, 6].

Early semantic segmentation approaches involved small datasets and few classes. Improved methodology and computing power led to larger, more diverse datasets with more complex taxonomies [7, 8, 1]. This development has provided valuable feedback that led to the current state of research where most of these datasets are about to be solved in the strongly supervised setup.

Despite the hard selection and annotation work, most existing datasets are still an insufficient proxy for real-life operation, even in a very restricted scenario such as road driving. For instance, none of the 20000 images from the Vistas dataset [1] include persons in non-standard poses, crashed vehicles or rubble. Additionally, real-life images may also be degraded due to hardware faults, inadequate acquisition, or lens distortion [9]. This suggests that foreseeing every possible situation may be an elusive goal and indicates that algorithms should be able to recognize image regions foreign to the training distribution [5].

These considerations emphasize the need to further improve the next generation of datasets. New datasets should contain atypical images which are likely to fool the current generation of models [9, 10]. Additionally, they should also endorse open-set evaluation [11] where the models are required to perform inference on arbitrary images. An open-set model is not supposed to predict an exact visual class in outliers. That would often be impossible since the exact visual class may not be present in the training taxonomy. Instead, it should suffice that outliers are recognized as such. The desired test subsets should contain various degrees of domain shift with respect to the training distribution. This should include diverse contexts (e.g. adverse weather, exotic locations) [1], exceptional situations (e.g. accidents, poor visibility) [9], and outright outliers (foreign domain objects and entire images) [9, 12]. Currently, there are only two such benchmarks in the dense prediction domain: WildDash [9] and Fishyscapes [12].

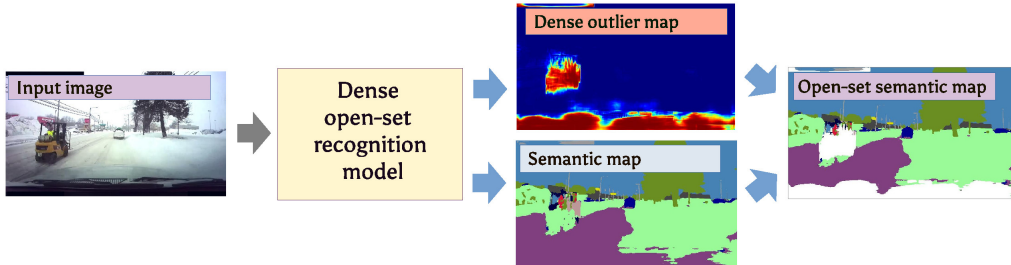


Figure 1: A dense open-set recognition model has to predict: i) a dense outlier map, and ii) a semantic map with C inlier classes. The merged open-set semantic map (right) contains outlier pixels (white) on two objects which are foreign to the training taxonomy: the ego-vehicle and the forklift.

This paper addresses dense open-set recognition and outlier detection as illustrated in Figure 1. Unlike previous [5] and concurrent [4] work, we propose to include test-agnostic noisy negatives to the training dataset. We believe that this setup is adequate due to extremely large capacity of deep models, which allows them to classify outliers into any class without hurting empirical accuracy in inliers [13]. We believe that our approach will represent a strong baseline for some time. It is very hard to bound the output of a deep model in foreign samples since they may have almost identical latent representations to some inliers. This holds true even for the current state-of-the-art generative models [6].

Our contribution is as follows. We propose a novel approach for dense outlier detection based on discriminative training with noisy negative images from a very large and diverse test-agnostic dataset. We show that successful operation in dense prediction context requires random pasting of negative patches to inlier training images. Our approach can share features with a closed-set semantic segmentation model. This greatly improves outlier detection while only slightly impairing semantic segmentation. Evaluation on two rigorous benchmarks and several other datasets indicates that our approach outperforms the state of the art [5, 10, 12, 4], especially on large outliers. In datasets with small outliers (FS Lost and Found), we achieve the best results complementing our approach with the max-softmax baseline.

Earlier accounts of this research appeared in [14, 15]. We extend our previous work with improved training procedure, broader experimental evaluation, and better results. Our consolidated experiments evaluate performance on established dense open-set benchmarks (WildDash

1 [9], Fishyscapes Static and Fishyscapes Lost and Found [12]), the StreetHazard dataset [10], and the proposed WD-Pascal dataset [14, 15]. Our experiments show that the proposed approach is broadly applicable without any dataset-specific tweaking. All our experiments use the same negative dataset and involve the same hyper-parameters. The resulting models produce dense open-set prediction with a single forward pass, which makes them suitable for real-time inference.

2. Related work

Open-set recognition combines classification and outlier detection. Some novelty detection approaches can be viewed as open-set recognition though this connection is seldom discussed. We are especially concerned with dense open-set recognition and focus on approaches that train on negative data.

2.1. Open-set recognition

Open-set recognition involves C known classes during training and $(C+1)$ classes during inference. The $(C+1)$ st label signifies that the sample does not belong to the training distribution. Outliers are usually recognized by thresholding some kind of score.

Open-set classification can be formulated on top of a classic closed-set discriminative model by estimating the outlier score from the prediction itself. Most recent work considers the probability of the winning class, also known as max-softmax (MSM) [16]. Unfortunately, deep models usually have highly confident outputs regardless of the input [17]. Different strategies can make max-softmax more informative, e.g. recalibration [17], preprocessing [18], MC-Dropout [19] or ensembling [20]. However, recalibration cannot improve average precision (AP). Preprocessing and MC-dropout offer only slight improvements over the baseline. MC-Dropout and ensembling require multiple forward passes, which may not be acceptable for large images and real-time inference.

Prediction uncertainty can also be assessed with a jointly trained head of the compound model. The two heads operate on shared features for efficiency and cross-task synergy [21, 5, 22]. Unfortunately, this can only recognize aleatoric uncertainty [5] which may arise due to inconsistent labels. Instead, outlier detection is related with epistemic uncertainty which arises due to insufficient learning [5, 23]. Epistemic uncertainty has been assessed under assumption that MC dropout approximates Bayesian model sampling [24]. However, that assumption may not be satisfied in practice. Additionally, existing approaches [5, 24] confound model uncertainty with distributional uncertainty [25].

We are especially interested in approaches which exploit negative samples during training. Most of these approaches complement the standard discriminative loss with a term which encourages high entropy in negative samples, such as KL-divergence towards a suitable prior [26, 27, 25]. A negative dataset can also be exploited to train a separate prediction head which directly predicts the outlier probability [14]. However, these approaches are sensitive to the choice of the negative dataset. An alternative approach trains on synthetic negatives which are generated at the border of the training distribution. However, experiments suggest that diverse negative datasets lead to better outlier detection than synthetic negative samples [26, 27].

2.2. Novelty detection

Novelty detection is an umbrella term which covers anomaly, rare-event, outlier and OOD detection, and one-class classification. Most of this work addresses generative models which attempt to model the training distribution. Anomalous examples should yield low probabilities in this setup, though this is difficult to achieve in practice [6, 28]. Generative adversarial networks can be used to score the difference between the input and the corresponding reconstruction [29] if the generator is formulated as an auto-encoder where the latent representation mapping is trained simultaneously alongside the GAN [30]. However, the obtained reconstructions are usually imperfect regardless of the type of input [20].

Several works emphasize contribution of knowledge transfer [20], although fine-tuning gradually diminishes pre-training benefits due to forgetting. This effect can be somewhat attenuated with a modified loss [31].

2.3. Dense open-set recognition

Dense open-set recognition is still an under-researched field despite important applications in intelligent transportation [3] and medical image analysis [4]. Some of the described novelty detection methods are capable of dense inference [20], however they address simple datasets and do not report pixel-level metrics. Hence, it is unclear whether they could be efficiently incorporated into competitive semantic segmentation frameworks.

Many image-wide open-set approaches can be adapted for dense prediction straightforwardly [5, 15, 12] though they are unable to achieve competitive performance due to many false positive outlier detections. This likely occurs because dense prediction incurs more aleatoric uncertainty than image-wide prediction due to being ill-posed at semantic borders [14].

A concurrent approach [12] fits an ensemble of normalized flows to latent features of the segmentation model. They infer negative log likelihoods in different layers and threshold with respect to the most likely activation across all layers. This approach achieves a fair accuracy on the Fishyscapes benchmark, however our submission outperforms it.

Preceding discussions suggest that dense open-set recognition is a challenging problem, and that best results may not be attainable by only looking at inliers. Our work is related to two recent image-wide outlier detection approaches which leverage negative data. Perera et al. [31] learn features for one-class classification by simultaneously optimizing cross-entropy on ImageNet images and feature compactness on the target images. However, inlier compactness and template-matching are not suitable for complex training ontologies. Hendrycks et al. [27] train a discriminative classifier to output low confidence in negative images. However, our experiments suggest tendency towards false positives due to aleatoric uncertainty at semantic borders.

Our work is also related to the dense open-set recognition approach which treats outlier detection by extending the inlier ontology [32]. The proposed composite dataset (MSeg) collects almost 200 000 densely annotated training images by merging public datasets such as Ade20k, IDD, COCO etc. Currently, this is the only approach that outperforms our submission to the WildDash 1 benchmark. However, the difference in performance is only 1.4pp although we train on smaller resolution (768 vs 1024) and use less negative supervision during training (bounding boxes from ImageNet-1k instead of dense labels on COCO, Ade20k and SUN RGB-D). Their approach does not appear on the Fishyscapes leaderboard.

3. Method

The main components of our approach are the dense feature extractor and the open-set recognition module illustrated in Fig. 2. The dense feature extractor is a fully convolutional module which transforms the input image $H \times W \times 3$ into a shared abstract representation $H/4 \times W/4 \times D$ where D is typically 256. The dense open-set recognition module incorporates recognition and outlier detection. We base these two tasks on shared features to promote fast inference and cross-task synergy [21, 31]. Our method relies on the following two hypotheses: i) training with diverse noisy negatives can improve outlier detection across various datasets, and ii) shared features greatly improve outlier detection without significant deterioration of semantic segmentation.

3.1. Dense feature extraction

Our feature extraction module consists of a powerful downsampling path responsible for semantics, and a lean upsampling path which restores the spatial detail. The downsampling path starts with a pre-trained recognition backbone. In case of DenseNet-169 it consists of four densely connected blocks (DB1-DB4) and three transition layers (T1-T3). Lightweight spatial pyramid pooling (SPP) provides wide context information [33, 34]. The upsampling path consists of three upsampling modules (U1-U3) which blend low resolution features from the previous upsampling stage with high-resolution features from the downsampling path. The resulting encoder-decoder structure is asymmetric. It has dozens of convolutional layers in the downsampling path and only three convolutional layers along the upsampling path [35]. We speed-up and regularize the learning with auxiliary cross-entropy losses. These losses target soft ground truth distribution across the corresponding window at full resolution [33].

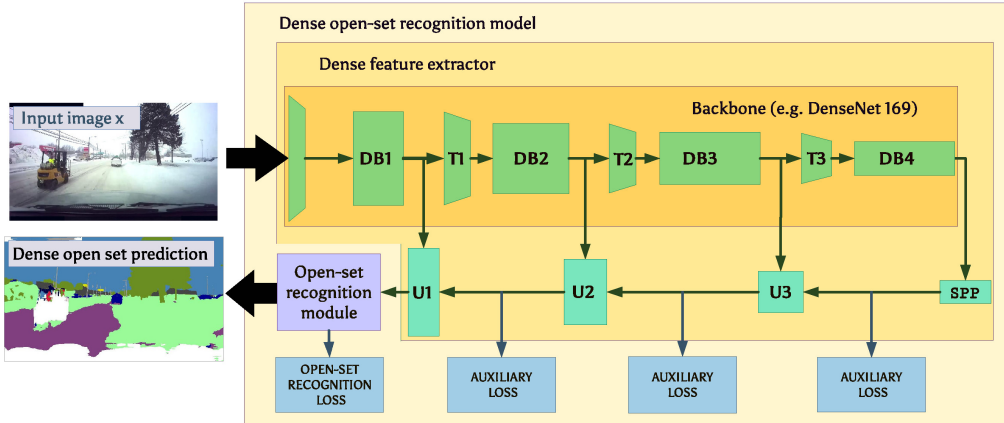


Figure 2: The proposed dense open-set recognition model consists of a dense feature extractor and a dense open-set recognition module. The dense feature extractor contains densely connected blocks (DB), transition blocks (T), spatial pyramid pooling layer (SPP) and lightweight upsampling blocks (U) [33]. We use auxiliary cross-entropy losses to speed-up and regularize training. The open-set recognition module produces semantic segmentation into $C+1$ classes, where the $C+1$ st class is the outlier class.

3.2. Two-head recognition module

We consider dense open-set recognition with shared features. We assume that the training data \mathcal{D} contains both inlier and noisy negative pixels. We denote images with \mathbf{x} , dense semantic predictions with \mathbf{Y} and the corresponding C-way ground truth labels with \mathbf{y} . Similarly, dense outlier predictions and the corresponding ground truth labels are \mathbf{O} and \mathbf{o} , respectively. We use i and j to denote the location of pixels. Most considerations become applicable to image classification by removing summation over all pixels (i,j) and regarding Y_{ij} and O_{ij} as image-wide predictions.

We propose a two-head open set recognition module which simultaneously emits dense closed-set posterior over classes $P(Y_{ij}|\mathbf{x})$, as well as the probability $P(O_{ij}|\mathbf{x})$ that the pixel at coordinates (i, j) is an outlier. Standard cross-entropy losses for the two predictions are as follows:

$$\begin{aligned} \mathcal{L}_{\text{cls}} &= - \sum_{\mathbf{x}, \mathbf{y}, \mathbf{o} \in \mathcal{D}} \sum_{ij} [\![o_{ij} = 0]\!] \cdot \log P(Y_{ij} = y_{ij}|\mathbf{x}) , \\ \mathcal{L}_{\text{od}} &= - \sum_{\mathbf{x}, \mathbf{o} \in \mathcal{D}} \sum_{ij} \log P(O_{ij} = o_{ij}|\mathbf{x}) . \end{aligned} \quad (1)$$

Figure 3 shows that equation 1 can be implemented as a multi-task model with shared features where the first head predicts semantic segmentation, while the second detects outliers.

Outlier detection overrides closed-set recognition when the outlier probability is over a threshold. Thus, the classification head is unaffected by negative data, which may preserve the baseline recognition accuracy even when training on test-agnostic negatives which are bound to be noisy.

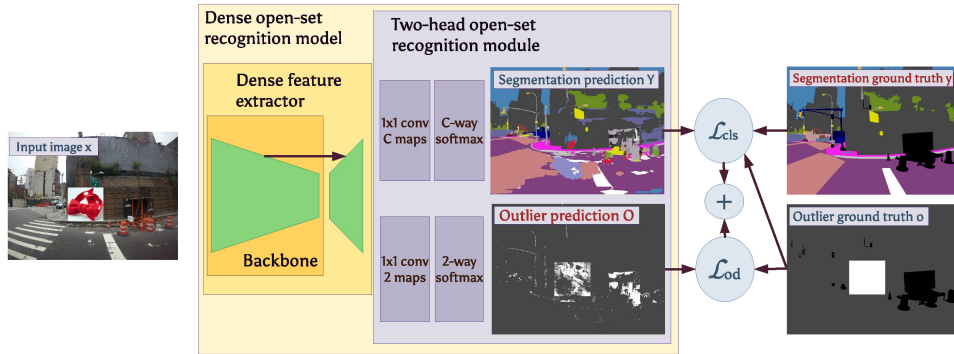


Figure 3: The architecture of the proposed two head open-set recognition module. The outlier detection head is a binary classifier which we train using the outlier ground truth. The segmentation head is a C-way classifier which requires both the segmentation and the outlier ground truth. The outlier ground truth is required for segmentation training in order to be able to exclude outlier pixels from \mathcal{L}_{cls} .

3.3. Exploiting noisy negatives

We propose to train our model by sampling negative data from an extremely diverse test-agnostic dataset such as ImageNet-1k. We observe that such dataset will necessarily overlap with inliers. For example, ImageNet-1k contains many classes from road-driving ontologies

used in Cityscapes [8] and Vistas [1] (e.g. cab, streetcar). Additionally, most stuff classes from Cityscapes (e.g. building, vegetation) are a regular occurrence in ImageNet-1k backgrounds. We refer to this issue as label noise.

We promote resistance to label noise by training on mixed batches with approximately equal share of inlier and negative images. Hence, inlier pixels in negative images are vastly outnumbered by true inliers for each particular class. We perform many inlier epochs during one negative epoch, since our negative training dataset is much larger than our inlier datasets. Our batch formation procedure prevents occasional inliers from negative images to significantly affect the training and favours stable development of batchnorm statistics. Unlike [12], we refrain from training on pixels labeled with the ignore class since we wish to use the same negative dataset in all experiments.

Our early experiments involved training on whole inlier images and whole negative images. The resulting models would work very well on test images with all inliers or all outliers. However, the performance was poor in images with mixed content [14]. It appears that the outlier detection head must be explicitly trained for mixed inputs to correctly generalize in such cases. We address this issue by pasting negative images into inlier images during training. We first resize the negative image to a small percent of the inlier resolution, and then paste it at random in the inlier image as illustrated in Figure 4. Subsequently, our models became capable of detecting outliers in inlier context [15]. We obtain the best results when the size of pasted patches is randomly chosen from a wide interval.

4. Experimental setup

Our open-set recognition models aim at achieving robustness with respect to various forms of distributional uncertainty [25]. Consequently all our experiments evaluate on datasets which are in some way different than the training ones.

4.1. Training datasets

We train our models on inliers from Cityscapes train [8], Vistas train [1], and StreetHazard train [10]. We train all our models on the same noisy negative training dataset which we refer to as ImageNet-1k-bb [15]. We collect ImageNet-1k-bb by picking the first bounding box from the 544546 ImageNet-1k images with bounding box annotations. We train on standalone negative images and mixed-content images obtained by pasting a resized negative image into an inlier crop. We resize each negative image to the desired share s_n of the inlier resolution, where the default is $s_n=5\%$. Models with the RSP suffix (randomly scaled patches) pick a random $s_n \in [0.1\%, 10\%]$ for each negative training image.

4.2. Validation dataset

Several previous approaches propose to evaluate dense open-set recognition on splits of existing real datasets that contain some visual classes which are absent from the training split. Thus, the BDD-Anomaly dataset [10] collects all BDD images without trains and motorcycles into the training split, and places all other BDD images into the test split. Cityscapes-IDD [36] proposes training on Cityscapes, and evaluating on cars (inliers) and rickshaws (outliers) from the IDD dataset. However, this approach is not easily carried out in practice since it is hard to avoid similarities between inlier and outlier classes. For instance, trains and motorcycles are similar to buses and bicycles, respectively, which are inliers in BDD-Anomaly. Similarly, rickshaws

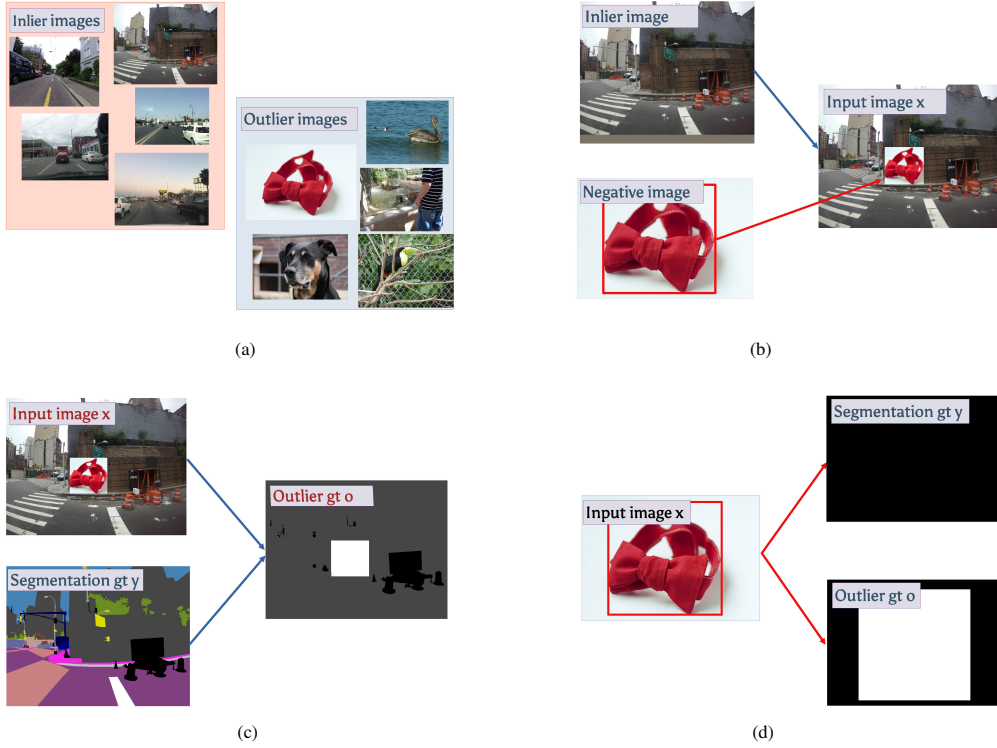


Figure 4: We train on images from the target dataset and noisy negatives from ImageNet-1k (a). We paste a randomly rescaled noisy negative bounding box into each positive training image (b). The pasted pixels are labeled as outliers (white) in the outlier detection ground truth (c). Negative training images are completely ignored by the semantic segmentation loss (black) and labeled as outliers only within the bounding box (d).

(Cityscapes-IDD outliers) are similar to motorcycles and cars (Cityscapes-IDD inliers). We attempt to avoid this pitfall by making sure that anomalies come from a different domain. We craft WD-Pascal [14] by randomly pasting Pascal animals into WildDash 1 val images. We select animals which take up at least 1% of the WildDash resolution. Conversely, we craft WD-LSUN by complementing WildDash 1 val with random subsets of LSUN [37] images, so that the number of inliers (WildDash 1) and outliers (LSUN) is approximately equal. We reduce the variance of all our validation and ablation experiments by averaging 50 assays across WildDash 1.

4.3. Evaluation datasets

We evaluate our models on several test dataset for dense open-set recognition. Our experiments report the outlier detection performance (AP, FPR_{95} [16]) and semantic segmentation accuracy (mIoU). The WildDash 1 benchmark [9] collects difficult road driving scenarios and negative images from other domains, but does not include images of mixed content. The Fishyscapes benchmark [12] includes Cityscapes images with pasted Pascal VOC objects. It also includes a subset of the Lost and Found dataset [38] where the outliers correspond to small obstacles on the road. The StreetHazards dataset [10] contains fully synthetic road-driving images while out-of-domain objects correspond to anomalies.

4.4. Implementation details

Our models are based on DenseNet-169 with ladder-style upsampling [33] as described in 3.1 due to best overall validation performance [15]. We normalize all images with ImageNet mean and variance. We denote the image size as its shorter dimension. We resize WD-Pascal and WD-LSUN images to 512 pixels. In all other experiments we resize validation and test images to 768 pixels. Some experiments train with scale jittering so that 30% images are resized to 512 pixels, while the remaining 70% images are randomly resized between 512 and 1536 pixels. We denote such models with the JS suffix (jittered scale). We form training batches with random 512×512 crops which we jitter with horizontal flipping. We do not use multi scale evaluation in order to report performance which could be delivered in real-time. We use the standard Adam optimizer and divide the learning rate of pre-trained parameters by 4. We validate the loss weights of all open-set recognition modules on a small subset of WD-Pascal. We train our two-head models with the compound loss $\mathcal{L}_{th} = 0.6\mathcal{L}_{cls} + 0.6 * 0.2\mathcal{L}_{od} + 0.4\mathcal{L}_{aux}$. We validate all hyper-parameters on WD-Pascal and WD-LSUN [15]. We train our models throughout 75 Vistas epochs, which corresponds to 5 epochs of ImageNet-1k-bb. This was increased to 20 epochs for our benchmark submissions. We detect outliers by thresholding inlier probability at $P(O_{ij} = 0|\mathbf{x})=0.5$.

5. Results

We validate mIoU accuracy on WildDash 1 val and outlier detection AP on WD-Pascal, WD-LSUN and Fishyscapes Lost and Found. We evaluate our models on the WildDash 1 benchmark, the Fishyscapes benchmark, and on the test subset of the StreetHazard dataset.

5.1. Validation of Dense Outlier Detection Approaches

Table 1 validates our method against several other dense open-set recognition approaches on WD-Pascal and WD-LSUN. All models have been trained on positive images from the Vistas dataset. Section 1 of the table presents models which are trained without negatives. We show the performance of max-softmax [16], max-softmax after ODIN [18] epistemic uncertainty after 50 forward passes with MC-Dropout [24], and densely trained confidence [21] (cf. Figure 5a).

The remaining models use noisy negatives from ImageNet-1k-bb during training. Section 2 of the table evaluates a single-task outlier detection model. The model performs better than the models from section 1, but much worse than models from section 4 which share features between the segmentation and the outlier detection tasks. This confirms our hypothesis that semantic segmentation loss forces the model to learn features which generalize well for outlier detection.

Section 3 evaluates the two-head module approach from Figure 3 when it is trained on whole inlier and whole negative images. This model is able to detect outlier images but it performs badly on images with mixed content. This shows that training with pasted negatives is a prerequisite for detecting outlier objects in front of an inlier background.

Section 4 of the table compares different open-set recognition modules which train on pasted noisy negatives from ImageNet-1k-bb as explained in 3.3. The two-head module architecture is illustrated in Figure 3, while the other three variants are illustrated in Figure 5. The C-way multi-class approach trains the model to emit low max-softmax in outlier samples [18, 26, 27] (Figure 5b). The C+1-way multi-class model performs prediction over C+1 classes, where the C+1st class is the outlier class (Figure 5c). Finally, the C-way multi-label approach trains C independent heads with sigmoidal activation (Figure 5d). Comparison with the top section clearly

| Model | AP WD-LSUN | AP WD-Pascal | mIoU WD |
|-------------------------------|-------------------|-------------------|-------------|
| C× multi-class | 55.6 ± 0.8 | 5.0 ± 0.5 | 50.6 |
| C× multi-class, ODIN | 56.0 ± 0.8 | 6.0 ± 0.5 | 51.4 |
| C× multi-class, MC | 64.1 ± 1.0 | 9.8 ± 1.2 | 48.4 |
| confidence head | 54.4 ± 0.8 | 3.4 ± 0.4 | 46.4 |
| single outlier detection head | 99.3 ± 0.0 | 15.0 ± 3.8 | N/A |
| two heads, no pasting | 98.9 ± 0.0 | 3.5 ± 0.6 | 46.27 |
| two heads(=LDN_BIN) | 99.3 ± 0.0 | 34.9 ± 6.8 | 47.9 |
| C× multi-class(=LDN_OE) | 99.5 ± 0.0 | 33.8 ± 5.1 | 47.8 |
| C+1× multi-class | 98.9 ± 0.1 | 25.6 ± 5.5 | 46.2 |
| C× multi-label | 98.8 ± 0.1 | 49.1 ± 5.6 | 43.4 |

Table 1: Validation of dense outlier detection approaches. WD denotes WildDash 1 val, MC denotes models trained and evaluated using Monte-Carlo dropout.

confirms our hypothesis that training with diverse noisy negatives can substantially improve outlier detection. We also note a slight reduction of the segmentation score in the column 4. This reduction is the lowest for the C-way multi-class model and the two-head model.

A closer inspection of models trained with noisy negatives shows that the C+1-way multi-class model performs the worst. The multi-label model performs well on outlier detection but quite poorly on inlier segmentation. The two-head model and the C-way multi-class model perform quite similarly, though further qualitative analysis shows that they differ in the type of errors they produce. The two-head model is more sensitive to domain shifts between the training and the validation sets while the C-way multi-class approach generates false positive outliers due to low max-softmax score at semantic borders.

5.2. Dense open-set recognition on WildDash 1 benchmark

Table 2 presents open-set recognition results on the WildDash 1 benchmark. Our models are listed in the last three rows of the table. The LDN_OE model has a single C-way multi-class head and uses max-softmax for outlier detection. The LDN_BIN and LDN_BIN_{JS} models have separate heads for semantic segmentation and outlier detection. The *JS* label indicates training with scale jittering. All three models have been trained on Vistas train, Cityscapes train, and WildDash 1 val (inliers) and ImageNet-1k-bb (noisy negatives).

LDN_BIN and LDN_OE differ only in open-set recognition modules, with the rest of the training setup being identical. The two-head model performs better in most classic evaluation categories as well as in the negative category, however it has a lower meta average score. This is caused by a larger performance drop in most hazard categories (more details can be found on the WildDash 1 web site).

LDN_BIN_{JS} has the same architecture as LDN_BIN but it is trained using scale jittering to be able to perform inference on larger resolutions (768x1451). This setup improves the segmentation accuracy across all categories and reduces sensitivity to hazards while slightly deteriorating performance in negative images. We did not retrain LDN_OE using scale jittering since this model produces false positives on semantic borders regardless of the inference resolution.

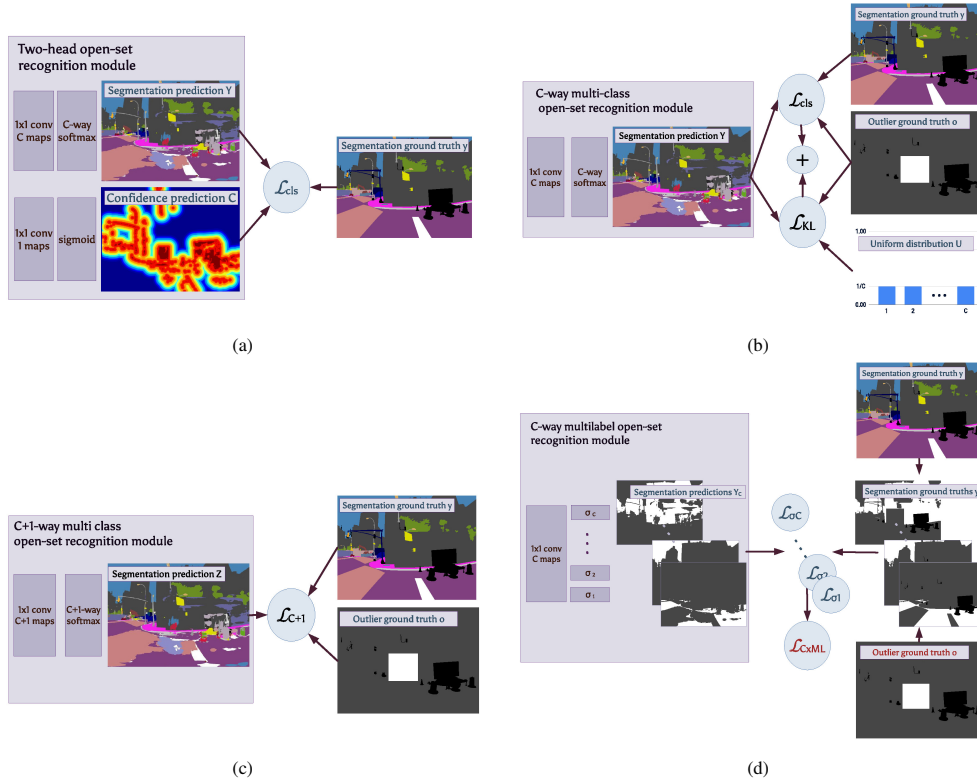


Figure 5: Four alternative open-set recognition modules. Two-head approach with trained confidence [21, 5] is similar to our approach in Figure 3, but it does not train on negative images (a). C-way multi-class approach [27, 26] learns uniform prediction in negative samples (b). C+1-way multi-class approach uses the negative data as a regular semantic class (c). C-way multi-label approach learns C one-versus-all classifiers [39] (d).

The best overall performance is achieved by the MSeg_1080 [32]. However, that model uses much more negative supervision: densely labeled Ade20k and COCO (they) vs bounding boxes from ImageNet-1k (us). Additionally, they train and evaluate on a larger resolution (1024 vs 768) and use a model with almost 4 times more parameters (65.8M vs 17.4M). Mseg_1080 is somewhat less sensitive to some hazards (most significantly underexposure) which may be due to a significantly larger inlier training dataset. Aside from Vistas and Cityscapes, they also use BDD (8000 images) and IDD (7974 images). On the other hand, MSeg does not use 70 images from WildDash 1 val. Our model is competitive and actually outperforms MSeg when evaluated on the same resolution (MSeg vs LDN_BIN).

Figure 6 presents a qualitative comparison between MSeg and LDN_BIN_{JS} as shown on the WildDash 1 benchmark. The columns show: i) original image, ii) MSeg output and iii) LDN_BIN_{JS} output. Images show that MSeg performs better on small objects and negative images which is likely due to larger resolution and more supervision. Note however that the MSeg model does not recognize black rectangles (row 2) as outliers. Detailed qualitative results for LDN_BIN and LDN_OE can be found in [15].

| Model | Meta Avg mIoU cla | Classic | | | | Negative mIoU cla |
|------------------------------|----------------------|-------------|-------------|-------------|-------------|----------------------|
| | | mIoU cla | iIoU cla | mIoU cat | iIoU cat | |
| DRN_MPC [40] | 28.3 | 29.1 | 13.9 | 49.2 | 29.2 | 15.9 |
| DeepLabv3+_CS [41] | 30.6 | 34.2 | 24.6 | 49.0 | 38.6 | 15.7 |
| MapillaryAI_ROB [42] | 38.9 | 41.3 | 38.0 | 60.5 | 57.6 | 25.0 |
| AHiSS_ROB [43] | 39.0 | 41.0 | 32.2 | 53.9 | 39.3 | 43.6 |
| MSeg [32] | 43.0 | 42.2 | 31.0 | 59.5 | 51.9 | 51.8 |
| MSeg_1080 [32] | 48.3 | 49.8 | 43.1 | 63.3 | 56.0 | 65.0 |
| LDN_BIN (ours) | 41.8 | 43.8 | 37.3 | 58.6 | 53.3 | 54.3 |
| LDN_OE (ours) | 42.7 | 43.3 | 31.9 | 60.7 | 50.3 | 52.8 |
| LDN_BIN _{JS} (ours) | 46.9 | 48.8 | 42.8 | 63.6 | 59.3 | 47.7 |

Table 2: Open-set segmentation results on the WildDash 1 benchmark

5.3. Open-set validation on Lost and Found dataset

Table 3 shows evaluation on the validation subset of Fishyscapes Lost and Found. All models were trained on inliers from Vistas train, Cityscapes train, and WildDash 1 val. LDN_{JS} denotes the max-softmax baseline trained with scale jittering and without outliers. All other models were also trained on noisy negatives from ImageNet-1k-bb. LDN_OE, LDN_BIN and LDN_BIN_{JS} are exact same models we submitted to the WildDash 1 benchmark. LDN_BIN_{JS, RSP} has the same architecture as LDN_BIN_{JS}, however it varies the size of pasted negatives during training in order to improve detection of smaller outliers. The last row combines our OOD head with max-softmax using multiplication. Later we show that this formulation succeeds since max-softmax complements our method when the outliers are very small

| Model | criterion | AP | AUROC | FPR95 | mIoU |
|----------------------------|-----------|-------------|-------------|-------------|-------------|
| LDN _{JS} | MSM | 7.8 | 92.1 | 26.6 | 76.4 |
| LDN_OE | MSM | 9.5 | 88.8 | 44.2 | 72.2 |
| LDN_BIN | OP | 13.2 | 88.0 | 71.9 | 75.1 |
| LDN_BIN _{JS} | OP | 25.4 | 89.8 | 90.0 | 76.5 |
| LDN_BIN _{JS, RSP} | OP | 36.9 | 96.1 | 20.0 | 76.3 |
| | OP × MSM | 45.7 | 95.6 | 24.0 | |

Table 3: Comparison of open-set segmentation approaches on Fishyscapes Lost and Found (AP, AUROC, FPR95(%)) and Vistas (mIoU) validation subsets. MSM is short for max-softmax, while OP stands for outlier probability estimated by the outlier detection head.

Both anomaly detection and semantic segmentation benefit from scale jittering during training. This is different than WildDash 1 where scale jittering decreased performance on negative images (cf. Table 2).

Figure 7 explores the influence of outlier size on model performance by plotting the relation between the outlier area and the detection performance. The figure shows AP and FPR95 with

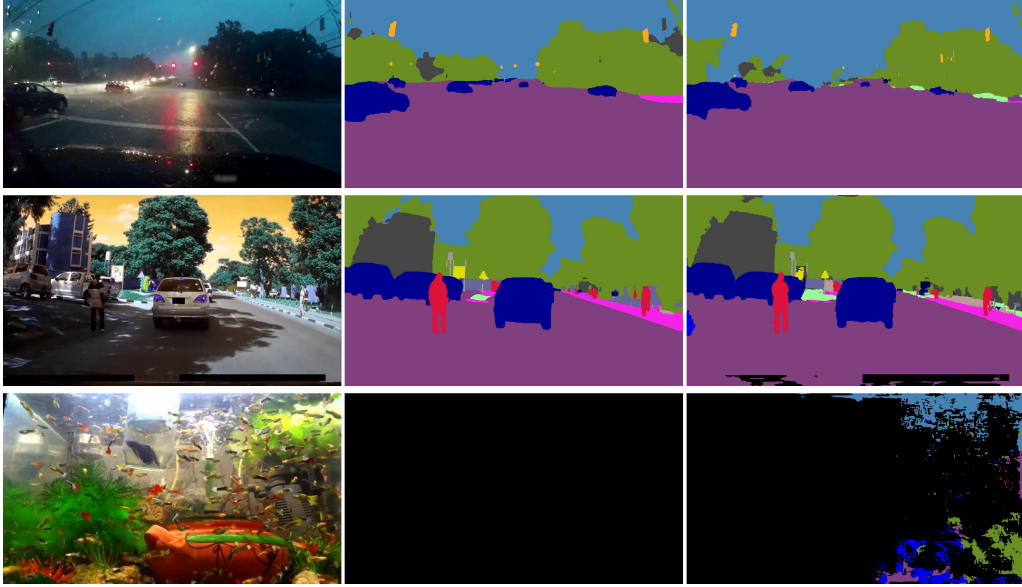


Figure 6: Qualitative comparison between MSeg (middle column) and LDN_BIN_{JS} (right column) on WildDash 1 test images (left column). MSeg performs better on some negative images (row 3), and small objects (row 1), but it appears unable to locate outlier patches in front of inlier background (row 2).

respect to the area of the outlier object for LDN_{JS} (which uses max-softmax for outlier detection), and LDN_BIN_{JS, RSP}. We see that the accuracy of both models depend on the size of the outlier. Max-softmax acts as an edge detector and therefore performs better on smaller objects. It however performs poorly on larger objects because it is unable to detect the interior of an object as an outlier.

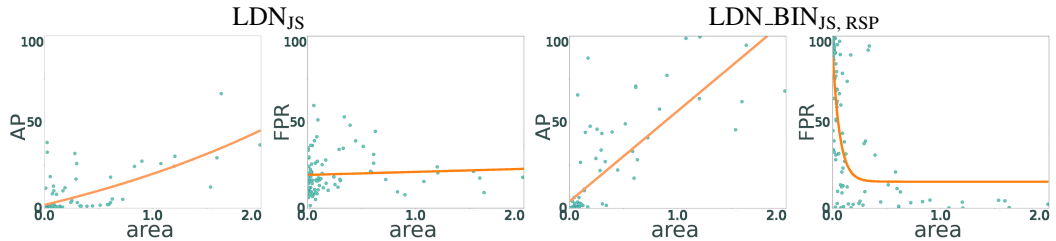


Figure 7: Influence of the outlier size on the model performance on Fishyscapes Lost and Found val. The two leftmost graphs show AP and FPR95 of the max-softmax baseline (LDN_{JS}) and the two rightmost graphs show AP and FPR95 for our model trained with noisy negatives (LDN_BIN_{JS, RSP}). Higher AP and lower FPR scores indicate that our model prevails on large outliers. Max-softmax on the other hand achieves better results on small outliers because it detects object edges well.

Figure 7 implies that we can improve the accuracy of our two head models on small objects by multiplying the outlier probability with max-softmax.

$$P(\text{outlier}_{ij}|x) = P(o_{ij} = 1|x) \cdot (1 - \max_c(P(y_{ijc}|x))) \quad (2)$$

This equation suggests that outliers should both appear strange to outlier detection head *and* produce small max-softmax scores. This formulation improves upon max-softmax by dampening outlier probabilities on semantic borders, since our trained outlier detection head perceives them as inliers. This formulation improves upon our trained outlier detection head on small outliers, since that is where max-softmax achieves fair performance.

Note that relatively poor performance of our model on small outliers does not come as a great surprise. Our predictions are 4 times subsampled with respect to the input resolution to reduce computational complexity and memory footprint during training. This is a common trade-off [44] which can be avoided, but at a great computational cost [45].

Figure 8 shows qualitative performance of our model. Column 1 presents the original image. Column 2 contains the ground truth, with inlier, outlier and ignore pixels denoted in gray, white and black respectively. Finally, column 3 shows the output of our LDN_BIN_{JS,RS P} model using a conjunction between our prediction and max-softmax probability (OD×MSP). Our model performs well on larger and closer objects (rows 1 and 3), while struggling with distant and small objects (rows 1 and 2). Finally, we note that some of the ignore pixels (e.g. ego-vehicle, noise on image borders) are also classified as anomalies.

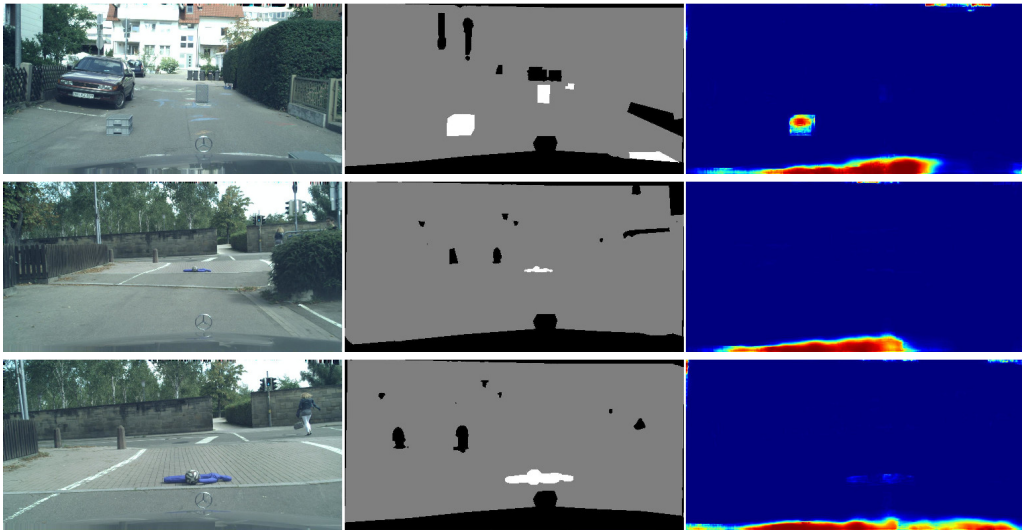


Figure 8: Outlier detection with LDN_BIN_{JS,RS P} and OP×MSM on Fishyscapes Lost and Found val. Columns present i) the original image, ii) the ground truth labels, and iii) the outlier probability. Our model works better on close objects than on distant ones (row 1). The outlier detection confidence grows as the camera draws nearer (rows 2, 3). Very small outliers are not detected (rows 1, 2).

5.4. Dense open-set recognition on the Fishyscapes benchmark

Table 4 shows current results on the Fishyscapes benchmark [12]. The benchmark provides segmentation accuracy on Cityscapes val, as well as outlier detection accuracy on FS Lost and Found and FS Static. FS Lost and Found comprises 300 images taken from the Lost and Found dataset. These images are relabelled to distinguish between inlier, outlier and void classes, and filtered to exclude road hazards which correspond to inlier classes (e.g. bicycles). FS static was created by pasting PASCAL VOC objects into Cityscapes images.

Note that $\text{LDN_BIN}_{\text{JS}}$ is almost exactly the same model that was presented in Table 2. Due to the requirement of the benchmark, the model had to be reimplemented in Tensorflow 1. We did not retrain the model, but reused the parameters learnt in Pytorch.

As in our validation experiments (see 5.3), $\text{LDN_BIN}_{\text{JS, RSP}}$ improves the detection of smaller outliers. This is reflected by an improved FPR95 score with respect to $\text{LDN_BIN}_{\text{JS}}$. The best results was achieved with $\text{LDN_BIN}_{\text{JS, RSP, ADE20K}}$ where instances from the ADE20K dataset were used as negatives during training. We outperform other models by a large margin on FS static. We also achieve the best FPR95 and a close second-best outlier detection AP on Lost and Found without significant drop in segmentation performance that occurs in the best submission.

| Model | Criterion | Train | OoD | City mIoU | Lost and Found | | FS Static | | |
|--|------------------------------------|--|----------|-------------|----------------|-------|-----------|-------------|-------------|
| | | | | | AP | FPR95 | AP | FPR95 | |
| Dirichlet DeepLab [12] | prior entropy | ✓ | ✓ | 70.5 | 34.3 | 47.4 | 31.3 | 84.6 | |
| Bayesian DeepLab [12] | mutual information | ✓ | ✗ | 73.8 | 9.8 | 38.5 | 48.7 | 15.5 | |
| OoD training [12] | maximize entropy | ✓ | ✓ | 79.0 | 1.74 | 30.6 | 27.5 | 23.6 | |
| Softmax [12] | entropy | ✗ | ✗ | 80.0 | 2.9 | 44.8 | 15.4 | 39.8 | |
| | max-softmax (MSM) | ✗ | ✗ | | 1.8 | 44.9 | 12.9 | 39.8 | |
| Learned embedding density [12] | logistic regression | ✗ | ✓ | 80.0 | 4.7 | 24.4 | 57.2 | 13.4 | |
| | minimum nll | ✗ | ✗ | | 4.3 | 47.2 | 62.1 | 17.4 | |
| | single-layer nll | ✗ | ✗ | | 3.0 | 32.9 | 40.9 | 21.3 | |
| Image resynthesis | resynthesis difference | ✗ | ✗ | 81.4 | 5.7 | 48.1 | 29.6 | 27.1 | |
| Discriminative outlier detection head (ours) | $\text{LDN_BIN}_{\text{JS}}$ | outlier probability (OP) | ✓ | ✓ | 77.7 | 15.7 | 76.9 | 82.9 | 5.1 |
| | $\text{LDN_BIN}_{\text{JS, RSP}}$ | outlier probability (OP) | ✓ | ✓ | 77.3 | 21.2 | 36.9 | 86.2 | 2.4 |
| | | OP × MSM | ✓ | ✓ | | 30.9 | 22.2 | 84.0 | 10.3 |
| | | $\text{LDN_BIN}_{\text{JS, RSP, ADE20K}}$ | OP × MSM | ✓ | ✓ | | 31.3 | 19.0 | 96.8 |

Table 4: Open-set segmentation evaluation on the Fishyscapes benchmark.

5.5. Open-set segmentation on StreetHazard

Table 5 presents open-set segmentation accuracy on StreetHazard. We evaluate the same models as in previous experiments (LDN_{JS} , $\text{LDN_BIN}_{\text{JS}}$ and $\text{LDN_BIN}_{\text{JS, RSP}}$) and compare them with the max-softmax baseline. We ignore outlier pixels when measuring segmentation accuracy. Unlike [10], we do not use ignore pixels during evaluation (same as [12]). Furthermore, we do not report the mean of per-image scores. In our view, such practice may yield over-optimistic estimate of the overall anomaly detection metrics, since recognition errors can not propagate across images. We therefore determine global scores on 10 times downsampled predictions. We evaluated the performance by measuring the mean of per-image scores and obtained similar results to the ones we report.

Figure 9 shows some qualitative results. The columns represent: i) the original image, ii) the ground truth and iii) our output.

6. Conclusion

We have presented a novel approach for dense outlier detection and open-set recognition. The main idea is to discriminate an application-specific inlier dataset (e.g. Vistas, Cityscapes), from a diverse general-purpose dataset (e.g. ImageNet-1k). Pixels from the latter dataset represent noisy test-agnostic negative samples. We train on mixed batches with approximately equal share

| model | criterion | AP | AUROC | FPR95 | test mIoU |
|----------------------------|-----------|--------------|--------------|-------------|--------------|
| PSPNet [10] | CRF+msm | 6.5 | 88.1 | 29.9 | N/A |
| PSPNet [46] | TRADI | 7.2 | 89.2 | 25.3 | N/A |
| LDN _{JS} | MSM | 7.28 | 87.63 | 38.13 | 65.04 |
| LDN_BIN _{JS} | OP | 18.56 | 87.00 | 79.08 | 66.32 |
| LDN_BIN _{JS, RSP} | OP | 19.74 | 88.86 | 56.19 | 66.94 |
| | OP×MSM | 18.82 | 89.72 | 30.86 | |

Table 5: Performance evaluation on StreetHazard

of inliers and noisy negatives. This promotes robustness to occasional inliers in negative images and favours stable development of batchnorm statistics. We encourage correct recognition of spatial borders between outlier and inlier pixels by pasting negative patches at random locations in inlier images. Consequently, the resulting models succeed to generalize in test images with mixed content. We have shown that feature sharing greatly improves dense outlier detection, while only slightly deteriorating semantic segmentation. The resulting multi-task architecture is able to perform dense open-set recognition with a single forward pass.

This is the first and currently the only method which competes at both dense open-set recognition benchmarks, Fishyscapes and WildDash 1. Currently, our model is at the top on Fishyscapes Static leaderboard, and a close runner-up on WildDash 1 while training with less supervision than the top rank algorithm [32]. The same model also achieves the runner-up AP and competitive FPR 95 on Fishyscapes Lost and Found. We achieve state-of-the-art AP accuracy on the Street-Hazard dataset despite a strong domain shift between our negative dataset (ImageNet-1k-bb) and the test dataset.

Our method outperformed the max-softmax baseline in all experiments. The advantage is greatest when the outliers are large, such as in Fishyscapes static and WildDash 1. A conjunction of our method and max-softmax becomes advantageous on Fishyscapes Lost and Found. This suggests that our method and max-softmax target independent traits of outlier pixels. Most reported experiments feature the same model, hyper parameters, training procedure, and the negative dataset: only the inliers are different.

The reported results confirm our hypotheses i) that noisy negatives can improve dense outlier detection and open-set recognition, and ii) that the shared features greatly improve outlier detection without significant deterioration of semantic segmentation. The resulting open-set models perform comparably with respect to their closed-set counterparts. Suitable directions for future work include improving our models on small outliers, as well as incorporating joint training with generative models.

Acknowledgment

This work has been supported by the Croatian Science Foundation under the grant ADEPT and the European Regional Development Fund under the grant DATACROSS.

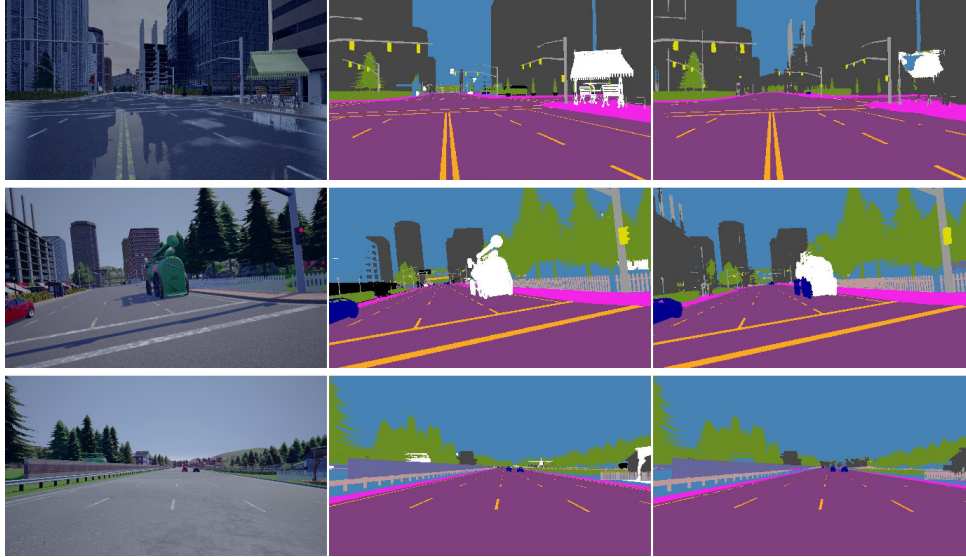


Figure 9: Open-set segmentation on StreetHazard. The columns show the input image, ground truth segmentation and the output of LDN_BINJS_RSP. Outliers are white while ignore pixels are black. Our model performs better on large outliers (rows 1, 2) than on small ones (row 3).

Published Paper

This manuscript has been accepted for publication Image and Vision Computing, after peer review and is subject to their terms of use, but is not the Version of Record and does not reflect post-acceptance improvements, or any corrections. The Version of Record is available here: <https://www.sciencedirect.com/science/article/pii/S0262885622001196>.

References

- [1] G. Neuhold, T. Ollmann, S. R. Bulò, P. Kotschieder, The mapillary vistas dataset for semantic understanding of street scenes, in: ICCV, 2017, pp. 5000–5009.
- [2] B. Zhou, H. Zhao, X. Puig, S. Fidler, A. Barriuso, A. Torralba, Scene parsing through ade20k dataset, in: CVPR, 2017, pp. 633–641.
- [3] P. Zhang, W. Liu, H. Wang, Y. Lei, H. Lu, Deep gated attention networks for large-scale street-level scene segmentation, Pattern Recognition 88 (2019) 702–714.
- [4] Y. Xia, Y. Zhang, F. Liu, W. Shen, A. Yuille, Synthesize then compare: Detecting failures and anomalies for semantic segmentation, in: ECCV, 2020.
- [5] A. Kendall, Y. Gal, What uncertainties do we need in bayesian deep learning for computer vision?, in: NIPS, 2017, pp. 5574–5584.
- [6] E. T. Nalisnick, A. Matsukawa, Y. W. Teh, D. Görür, B. Lakshminarayanan, Do deep generative models know what they don't know?, in: ICLR, 2019.
- [7] M. Everingham, L. Gool, C. K. Williams, J. Winn, A. Zisserman, The pascal visual object classes (voc) challenge, Int. J. Comp. Vis. 88 (2010) 303–338.
- [8] M. Cordts, M. Omran, S. Ramos, T. Rehfeld, M. Enzweiler, R. Benenson, U. Franke, S. Roth, B. Schiele, The cityscapes dataset for semantic urban scene understanding, in: CVPR, 2016, pp. 3213–3223.
- [9] O. Zendel, K. Honauer, M. Murschitz, D. Steininger, G. Fernandez Dominguez, Wilddash - creating hazard-aware benchmarks, in: ECCV, 2018, pp. 407–421.
- [10] D. Hendrycks, S. Basart, M. Mazeika, M. Mostajabi, J. Steinhardt, D. Song, A benchmark for anomaly segmentation, arXiv preprint arXiv:1911.11132 (2019).

- [11] W. Scheirer, L. Jain, T. Boult, Probability models for open set recognition, *IEEE Trans. Pattern Anal. Mach. Intell.* 36 (2014) 2317–2324.
- [12] H. Blum, P.-E. Sarlin, J. Nieto, R. Siegwart, C. Cadena, Fishyscapes: A benchmark for safe semantic segmentation in autonomous driving, in: *ICCVW*, 2019, pp. 2403–2412.
- [13] C. Zhang, S. Bengio, M. Hardt, B. Recht, O. Vinyals, Understanding deep learning requires rethinking generalization, in: *ICLR*, 2017.
- [14] P. Bevandic, I. Kreso, M. Orsic, S. Segvic, Discriminative out-of-distribution detection for semantic segmentation, *arXiv preprint arXiv:1808.07703* (2018).
- [15] P. Bevandic, I. Kreso, M. Orsic, S. Segvic, Simultaneous semantic segmentation and outlier detection in presence of domain shift, in: *GCPR*, 2019, pp. 33–47.
- [16] D. Hendrycks, K. Gimpel, A baseline for detecting misclassified and out-of-distribution examples in neural networks, in: *ICLR*, 2017.
- [17] C. Guo, G. Pleiss, Y. Sun, K. Q. Weinberger, On calibration of modern neural networks, in: *ICML*, 2017, pp. 1321–1330.
- [18] S. Liang, Y. Li, R. Srikant, Enhancing the reliability of out-of-distribution image detection in neural networks, in: *ICLR*, 2018.
- [19] Y. Gal, Z. Ghahramani, Dropout as a bayesian approximation: Representing model uncertainty in deep learning, in: *ICML*, 2016, p. 1050–1059.
- [20] P. Bergmann, M. Fauser, D. Sattlegger, C. Steger, Uninformed students: Student-teacher anomaly detection with discriminative latent embeddings, in: *CVPR*, 2020, pp. 4182–4191.
- [21] T. DeVries, G. W. Taylor, Learning confidence for out-of-distribution detection in neural networks, *arXiv preprint arXiv:1802.04865* (2018).
- [22] H. Zhang, A. Li, J. Guo, Y. Guo, Hybrid models for open set recognition, in: *ECCV*, 2020.
- [23] E. Hüllermeier, W. Waegeman, Aleatoric and epistemic uncertainty in machine learning: A tutorial introduction, *arXiv preprint arXiv:1910.09457* (2019).
- [24] L. Smith, Y. Gal, Understanding measures of uncertainty for adversarial example detection, in: *UAI*, 2018, pp. 560–569.
- [25] A. Malinin, M. Gales, Predictive uncertainty estimation via prior networks, in: *NeurIPS*, 2018, pp. 7047–7058.
- [26] K. Lee, H. Lee, K. Lee, J. Shin, Training confidence-calibrated classifiers for detecting out-of-distribution samples, in: *ICLR*, 2018.
- [27] D. Hendrycks, M. Mazeika, T. Dietterich, Deep anomaly detection with outlier exposure, in: *ICLR*, 2019.
- [28] W. Grathwohl, K. Wang, J. Jacobsen, D. Duvenaud, M. Norouzi, K. Swersky, Your classifier is secretly an energy based model and you should treat it like one, in: *ICLR*, 2020.
- [29] H. Zenati, M. Romain, C. Foo, B. Lecouat, V. Chandrasekhar, Adversarially learned anomaly detection, in: *ICDM*, 2018, pp. 727–736.
- [30] Y. Zhang, Y. Gong, H. Zhu, X. Bai, W. Tang, Multi-head enhanced self-attention network for novelty detection, *Pattern Recognit.* 107 (2020) 107486.
- [31] P. Perera, V. M. Patel, Learning deep features for one-class classification, *IEEE Transactions on Image Processing* 28 (2019) 5450–5463.
- [32] J. Lambert, L. Zhuang, O. Sener, J. Hays, V. Koltun, MSeg: A composite dataset for multi-domain semantic segmentation, in: *CVPR*, 2020, pp. 2876–2885.
- [33] I. Krešo, J. Krapac, S. Segvic, Efficient ladder-style densenets for semantic segmentation of large images, *IEEE Trans. Intell. Transp. Syst.* (2020) 1–11.
- [34] H. Zhao, J. Shi, X. Qi, X. Wang, J. Jia, Pyramid scene parsing network, in: *CVPR*, 2017, pp. 6230–6239.
- [35] I. Kreso, J. Krapac, S. Segvic, Ladder-style densenets for semantic segmentation of large natural images, in: *ICCV CVRSUAD*, 2017, pp. 238–245.
- [36] M. Angus, K. Czarnecki, R. Salay, Efficacy of pixel-level OOD detection for semantic segmentation, *arXiv preprint arXiv:1911.02897* (2019).
- [37] F. Yu, Y. Zhang, S. Song, A. Seff, J. Xiao, Lsun: Construction of a large-scale image dataset using deep learning with humans in the loop, *arXiv preprint arXiv:1506.03365* (2015).
- [38] P. Pinggera, S. Ramos, S. Gehrig, U. Franke, C. Rother, R. Mester, Lost and found: detecting small road hazards for self-driving vehicles, in: *IROS*, 2016, pp. 1099 – 1106.
- [39] G. Franchi, A. Bursuc, E. Aldea, S. Dubuisson, I. Bloch, One versus all for deep neural network incertitude (OVNNI) quantification, *arXiv:2006.00954* (2020).
- [40] F. Yu, V. Koltun, T. Funkhouser, Dilated residual networks, in: *CVPR*, 2017, pp. 636–644.
- [41] L.-C. Chen, Y. Zhu, G. Papandreou, F. Schroff, H. Adam, Encoder-decoder with atrous separable convolution for semantic image segmentation, in: *ECCV*, 2018, pp. 801–818.
- [42] S. R. Bulò, L. Porzi, P. Kotschieder, In-place activated batchnorm for memory-optimized training of dnns, in: *CVPR*, 2017, pp. 5639–5647.

- [43] P. Meletis, G. Dubbelman, Training of convolutional networks on multiple heterogeneous datasets for street scene semantic segmentation, in: IV, 2018, pp. 1045–1050.
- [44] O. Russakovsky, J. Deng, H. Su, J. Krause, S. Satheesh, S. Ma, Z. Huang, A. Karpathy, A. Khosla, M. Bernstein, A. C. Berg, L. Fei-Fei, ImageNet Large Scale Visual Recognition Challenge, *Inter. Jour. of Comput. Vision* 115 (2015) 211–252.
- [45] R. Zhu, S. Zhang, X. Wang, L. Wen, H. Shi, L. Bo, T. Mei, Scratchdet: Training single-shot object detectors from scratch, in: CVPR, 2019, pp. 2263–2272.
- [46] G. Franchi, A. Bursuc, E. Aldea, S. Dubuisson, I. Bloch, Tradi: Tracking deep neural network weight distributions, in: ECCV, 2020, pp. 105–121.